Seasonal and nonseasonal variability of satellite-derived chlorophyll and colored dissolved organic matter concentration in the California Current

Mati Kahru and B. Greg Mitchell

Scripps Institution of Oceanography, University of California, San Diego, La Jolla, California

Abstract. Time series of surface chlorophyll *a* concentration (Chl) and colored dissolved organic matter (CDOM) derived from the Ocean Color and Temperature Sensor and Sea-Viewing Wide Field-of-View Sensor were evaluated for the California Current area using regional algorithms. Satellite data composited for 8-day periods provide the ability to describe large-scale changes in surface parameters. These changes are difficult to detect based on in situ observations alone that suffer from undersampling the large temporal and spatial variability, especially in Chl. We detected no significant bias in satellite Chl estimates compared with ship-based measurements. The variability in CDOM concentration was significantly smaller than that in Chl, both spatially and temporally. While being subject to large interannual and short-term variations, offshore waters (100-1000 km from the shore) have an annual cycle of Chl and CDOM with a maximum in winter-spring (December-March) and a minimum in late summer. For inshore waters the maximum is more likely in spring (April-May). We detect significant increase in both Chl and CDOM off central and southern California during the La Niña year of 1999. The trend of increasing Chl and CDOM from October 1996 to June 2000 is statistically significant in many areas.

1. Introduction

The detailed spatial coverage provided by images from space-borne ocean color sensors has had a major impact on biological oceanography [e.g., McClain, 1993]. However, application of satellite data for detecting annual or long-term temporal variations is complicated owing to variations in the calibration coefficients, sensitivity. sensor atmospheric and viewing conditions, changes in the ocean's vertical stratification, and other potential caveats. Seasonality is one of the basic modes of variability in many ecosystems and, if present, should be detectable by satellite sensors. Previous studies of seasonal periodicity in surface chlorophyll a concentration (Chl) in the California Current using in situ or satellite data have drawn different conclusions [Strub et al., 1990; Thomas and Strub, 1990; Fargion et al., 1993].

With over 3 years of the combined Ocean Color and Temperature Sensor (OCTS) and Sea-Viewing Wide Field-of-View Sensor (SeaWiFS) data available, it is now possible to reevaluate the ocean color time series off California using data from these new sensors. The new ocean color sensors are expected to have improved radiometric accuracy and atmospheric correction algorithms compared with the Coastal Zone Color Scanner (CZCS) [McClain et al., 1998]. The increased number of spectral bands with higher-quality data also makes it possible to derive products other than chlorophyll that may provide additional insights into the functioning of the ecosystem. In this paper we analyze the time series of Chl and colored dissolved organic matter

Copyright 2001 by the American Geophysical Union

Paper number 1999JC000094. 0148-0227/01/1999JC000094\$09.00

(CDOM) derived from the OCTS and SeaWiFS data using regional and global algorithms and validate them using in situ data collected on the California Cooperative Oceanic Fisheries Investigations (CalCOFI) cruises [Mitchell and Kahru, 1998; Kahru and Mitchell, 1999].

2. Data and Methods

Time series in the California Current were evaluated in a grid of 3 by 4 individual subareas defined by three alongshore bands divided into four zones (Figure 1). For this article, the three bands parallel to the coastline are named "inshore" (within ≈100 km of the coast), "outer shelf" (100-300 km), and "offshore" (300-1000 km). The zone boundaries were defined by major coastal shelf and coastline features, including Cape Mendocino, Point Conception, the Ensenada front, Punta Eugenia, and Cabo San Lucas, which are known to have influence on the large-scale physical and biological interactions in the California Current [Bernal and McGowan, 1981; Chelton et al., 1982; Lynn and Simpson, 1987].

In situ data were collected on CalCOFI cruises between October 1996 and January 2000 [Hayward et al., 1999]. Chl was measured with the fluorometric method [Venrick and Hayward, 1984]. Spectral reflectance methods are described by Mitchell and Kahru [1998]. CDOM is operationally defined as the volume absorption coefficient at 300 nm of 0.2-µm filtered seawater relative to purified freshwater prepared at sea and was determined as described by Mitchell et al. [2000]. The concentration of CDOM in offshore California Current waters is low, and the experimental measurement error in the visible region is relatively large. Owing to the significantly better signal-to-noise ratio at shorter wavelengths, we selected the CDOM absorption

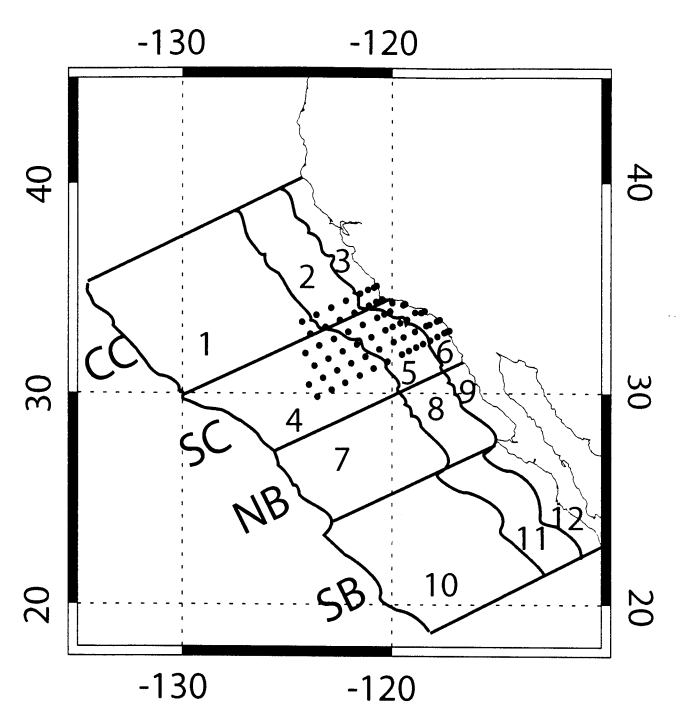


Figure 1. California Current study region with the grid of 3 by 4 subareas, numbered from 1 to 12. The alongshore bands are, from east to west, 0-100 km, 100-300 km, and 300-1000 km from the coastline, and the zones from north to south are named central California (CC), southern California (SC), northern Baja (NB), and southern Baja (SB).

coefficient ($a_{\rm CDOM}$) at 300 nm as an indicator of the CDOM concentration. Absorption by CDOM at other wavelengths can be derived from $a_{\rm CDOM}$ (300) and the exponential slope s of the spectral shape [e.g., $Bricaud\ et\ al.$, 1981]. The current CalCOFI station grid has significant coverage in our subareas 5 and 6. Some cruises covered a more limited station grid and had no optics or CDOM measurements. For validation of the satellite estimates, we use median values of Chl and CDOM in the top 10 m for each cruise, centered at the mean time when the ship measurements were taken.

Time series derived from satellite data were constructed using the statistical median for each of the 12 subareas. The median was preferred over the mean as it is less susceptible to outliers. At 9-km resolution the areas contained from 492 to 6691 pixels. Clouds often cover significant parts of images, and statistics over a few cloud-free pixels may not be representative for the whole subarea; therefore a subarea was considered to have no data if the number of valid pixels was less than 100.

OCTS imagery is available from October 1996 to June 1997, and SeaWiFS imagery is available from September 1997 to the present. No data are available during the approximately 2 months between the OCTS and SeaWiFS missions. Cloud cover and satellite orbit characteristics require compositing of satellite images over a period longer than 1 day to achieve meaningful statistics within each subarea. Time series of the normalized water-leaving radiances ($L_{\rm WN}$) were constructed from space-time binned (level 3) 9-km weekly OCTS (version 4) and 8-day SeaWiFS (reprocessing number 3) composites. For brevity, both of these time series will be referred to as "weekly." The time

series of Chl and CDOM were constructed from the weekly $L_{\rm WN}$ composites. In-water algorithms are nonlinear, therefore the use of binned radiances to derive other variables may lead to bias when compared with composites of the derived fields calculated from unbinned (level 2) data [Campbell et al., 1995]. In order to evaluate the errors caused by using the binned weekly $L_{\rm WN}$ data, we compared Chl and CDOM time series calculated from daily, weekly, and monthly binned $L_{\rm WN}$ images as well as with Chl time series constructed from the level 3 Chl composites provided by the National Space Development Agency of Japan (NASDA) and NASA.

For detecting periodicities in the time series, we calculated variance spectra using the multitaper method [Dettinger et al., 1995] and the Lomb normalized periodograms [Lomb, 1976; Press et al., 1992]. For detecting trends in the time series, the Sen slope estimator [Gilbert, 1987] was used in which one computes the slope between all pairs of points and estimates the overall trend as the median value. Confidence limits for the slope indicator were calculated as a simple percentile of the total number of calculated slopes.

Sea surface temperature (SST) time series were compiled from the advanced very high resolution radiometer (AVHRR) Pathfinder global data sets produced by the National Oceanic and Atmospheric Administration (NOAA) and NASA [Vazquez et al., 1995]. The mean annual SST cycle for each subarea was derived as an average of the monthly MCSST (1981-1986) and Pathfinder (1987-1999) data sets, and the SST anomalies were derived by subtracting the mean annual SST from the median monthly temperatures of each subarea.

3. Algorithms

Chl was derived using both empirical and semianalytic algorithms. The empirical algorithms included our regional CAL-P6 [Kahru and Mitchell, 1999] and the global OC2v2 and OC4v4 algorithms [O'Reilly et al., 1998, 2000; McClain et al., 1998]. CAL-P6 and OC2v2 use the $L_{\rm WN}$ (490)/ $L_{\rm WN}$ (555) band ratio to derive Chl and differ only in the form of the approximation. The CAL-P6 algorithm was developed exclusively with the California Current in situ data and is expected to be more accurate for this region. The satellitederived L_{WN} values may have errors as a consequence of atmospheric correction errors and other uncertainties. Therefore the accuracy of a satellite Chl estimate is dependent on many factors. The CAL-P6 algorithm tends to produce a higher coefficient of determination (r^2) and a smaller rootmean-square (RMS) error compared to the standard SeaWiFS algorithms OC2v2 [Kahru and Mitchell, 1999] and OC4v4 (Figure 2) when applied to our in situ versus satellite matchup data set. The standard SeaWiFS algorithms tend to underestimate Chl at concentrations from 1 to 10 mg m⁻³.

The standard OCTS Chl algorithm uses three $L_{\rm WN}$ bands [O'Reilly et al., 1998]. Comparison of the monthly averages over each sensor's lifetime in each of the subareas revealed that the standard OCTS version 4 Chl product from NASDA was similar at higher concentrations but significantly lower in comparison with SeaWiFS at low Chl. In oligotrophic areas, Chl concentration is expected to have minimal temporal and spatial variability, and no significant long-term trend in the in situ Chl has been observed [Kahru and Mitchell, 2000]. For a proper comparison between the sensors, we applied the CAL-P6 algorithm to both sensors. A modification of the CAL-P6

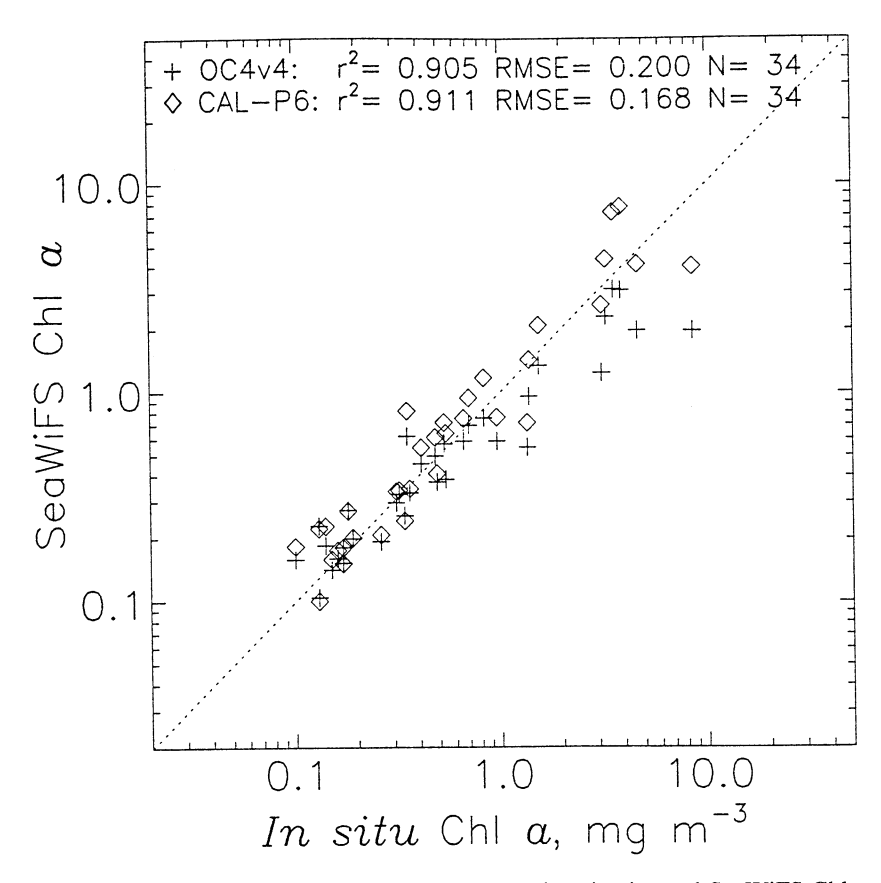


Figure 2. Comparison of the near-simultaneous (± 4 hours, ± 1 km) in situ and SeaWiFS Chl estimates. The high-resolution SeaWiFS data were processed with SeaDAS 4.0 with the default parameters. The log-log linear regression for the standard OC4v4 algorithm is: Y = -0.125 + 0.778 X. CAL-P6 algorithm was applied to the derived $L_{\rm WN}$ (490) and $L_{\rm WN}$ (555) values averaged in the corresponding 3 x 3 pixel window. The corresponding regression for CAL-P6 is Y = 0.048 + 0.991 X.

coefficients for OCTS was necessary for the slightly different spectral bands (565 nm on OCTS versus 555 nm on SeaWiFS). For developing algorithms using OCTS spectral bands not present in our in situ radiometers [Mitchell and Kahru, 1998], we estimated in situ values of spectral reflectance using cubic spline interpolation of the measured wavelengths. Since $L_{\rm WN}$ spectra are smooth for 10 to 20-nm bandwidths, the accuracy of the interpolations is expected to be comparable to the accuracy of the measured bands. The equation forms and coefficients of the algorithms are given in Table 1.

In contrast to the empirical band ratio algorithms, the Carder semianalytic algorithm [Carder et al., 1999] uses all five SeaWiFS $L_{\rm WN}$ bands (from 412 to 555-nm) and derives, among others, Chl and the absorption coefficient of the sum of CDOM and detrital matter (a_g) . The version of the Carder model used was v1p3 with the default parameter set as implemented in the SeaDAS 3.3 software [Fu et al., 1998]. The output of the Carder et al. [1999] semianalytic model, a_g , is the sum of the absorption by CDOM $(a_{\rm CDOM})$ and detrital particles (a_d) , which are difficult to separate optically. However, according to our CalCOFI data, a_d at 300 nm is only approximately 4.5% (median of 106 stations) of $a_{\rm CDOM}$ + a_d and therefore a_g (300) derived from the Carder model is dominated by $a_{\rm CDOM}$ (300). In the Carder algorithm the value of the exponential slope (s = 0.025) is a fixed parameter and

should not be used to extrapolate beyond the model wavelengths (K. Carder, personal communication, 1999). Therefore we used the average slope for the CalCOFI data set (s = 0.0185) to convert the output of the model $a_g(400)$ to $a_e(300)$.

Empirical band ratio algorithms for a_{CDOM} (300) were derived from our in situ data set. The band ratios used were L_{WN} (443)/ L_{WN} (520) for OCTS and L_{WN} (443)/ L_{WN} (510) for SeaWiFS (Figure 3a). Absorption by CDOM is strong at 443nm but weak at wavelengths greater than 500-nm with an exponential decrease with wavelength. Particulate absorption is rather strong from 500 to 520-nm, which is caused by accessory pigments that are well correlated with chlorophyll a. While empirical algorithms using 443-nm and 510- (520) nm bands are not fully independent of Chl variability, they provide a reasonably good index of CDOM. We deliberately avoided the use of L_{WN} (412) in our CDOM algorithm because of known problems with atmospheric correction at short wavelengths [Barnard et al., 1998; Kahru and Mitchell, 1999; Siegel et al., 2000]. The prediction accuracy of the CDOM band ratio model was similar ($r^2 = 0.77$) for both sensors. We believe that a significant portion of the scatter is due to the in situ measurement errors of both a_{CDOM} and L_{WN} . The algorithms and the numerical coefficients are given in Table 1. We validated our SeaWiFS CDOM algorithm with 11 direct match-ups of the satellite and in situ data collected

Variable	Algorithm	Type, Satellite	Equation, Coefficients a, Band Ratio R
CHLA	CAL-P6	6th-order polynomial	CHLA = $10 (a_0 + a_1*R + a_2*R^2 + a_3*R^3 + a_4*R^4 + a_5*R^5 + a_6*R^6)$
	[Kahru and Mitchell, 1999]	OCTS	$R = \log \left[L_{\text{WN}}(490)/L_{\text{WN}}(565) \right]$ a = [0.522, -2.247, -0.001, -1.970, 3.11, 4.844, -7.678]
		SeaWiFS	$R = \log [L_{WN}(490)/L_{WN}(555)]$ $a = [0.565, -2.561, -1.051, -0.294, 5.561, 3.130, -10.816]$
CDOM	CDOM	power law	$a_{\text{CDOM}}(300) = 10 (a_0 + a_1 * R)$
		OCTS	$R = \log \left[L_{\text{WN}}(443)/L_{\text{WN}}(520) \right]$ a = [-0.411, -0.703]
		SeaWiFS	$R = \log \left[L_{WN}(443)/L_{WN}(510) \right]$ $a = [-0.393, -0.872]$

Table 1. Formulations of the Empirical Chlorophyll (CHLA) and CDOM Algorithms for OCTS and SeaWiFS

within ± 4 hours of each other (Figure 3b). The RMS error of our SeaWiFS-derived estimate of $a_{\rm CDOM}$ (300) (19.7%, $r^2=0.81$) was considerably lower in comparison with the error when $a_{\rm CDOM}$ (300) was estimated from a correlation with the in situ Chl (RMS error, 81%; $r^2=0.56$). The Carder algorithm produced $a_{\rm g}(300)$ values that were also well correlated with in situ $a_{\rm g}(300)$ values ($r^2=0.70$), but it failed at 2 out of the 11 match-ups and significantly overestimated in situ $a_{\rm g}(300)$ (regression slope, 2.62). This overestimate is due in part to low $L_{\rm WN}$ (412) in the SeaWiFS data.

4. Time Series

4.1. Normalized Water-Leaving Radiance

 $L_{\rm WN}$ (443) and $L_{\rm WN}$ (490) were common for both sensors, while other bands used in the Chl and CDOM algorithms had

slight spectral differences. The OCTS L_{WN} (490) variability was very similar in comparison with SeaWiFS, but the OCTS $L_{\rm WN}$ (443) values tended to be higher in comparison with the same SeaWiFS band (Figure 4). No direct comparison is possible because the sensors' operations did not overlap. While the NASDA calibration of the OCTS is in good agreement with independent vicarious calibration [Wang et al., 1999], systematic bias between the sensors cannot be ruled out considering the different sensor characteristics. calibration methods, and atmospheric correction algorithms. From SeaWiFS reprocessing number 2 to reprocessing number 3, L_{WN} (555) increased by about 5-15% owing to changes in the processing code and coefficients, while changes in other L_{WN} bands were minor. The effect of the increased $L_{\rm WN}$ (555) was an increase in the derived Chl concentration. It is not within the scope of this paper to

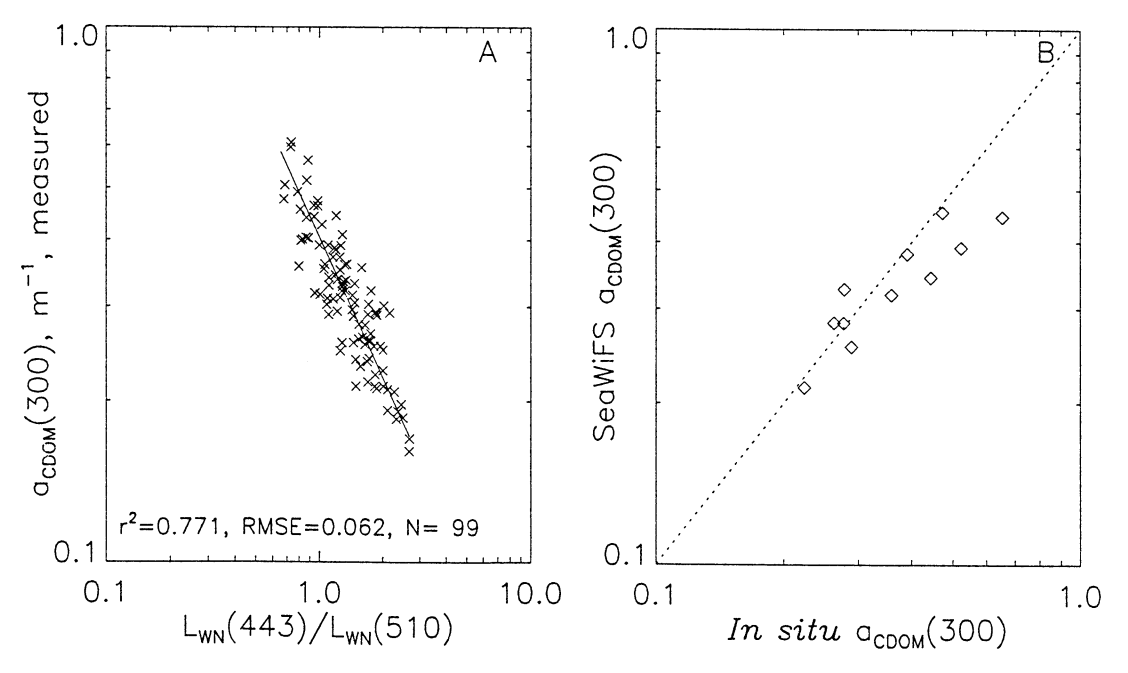


Figure 3. (a) Band ratio algorithm used for deriving CDOM from the in situ water-leaving radiances and (b) a validation based on near-simultaneous (± 4 hours, ± 1 km) SeaWiFS and in situ data (N = 11, $r^2 = 0.81$).

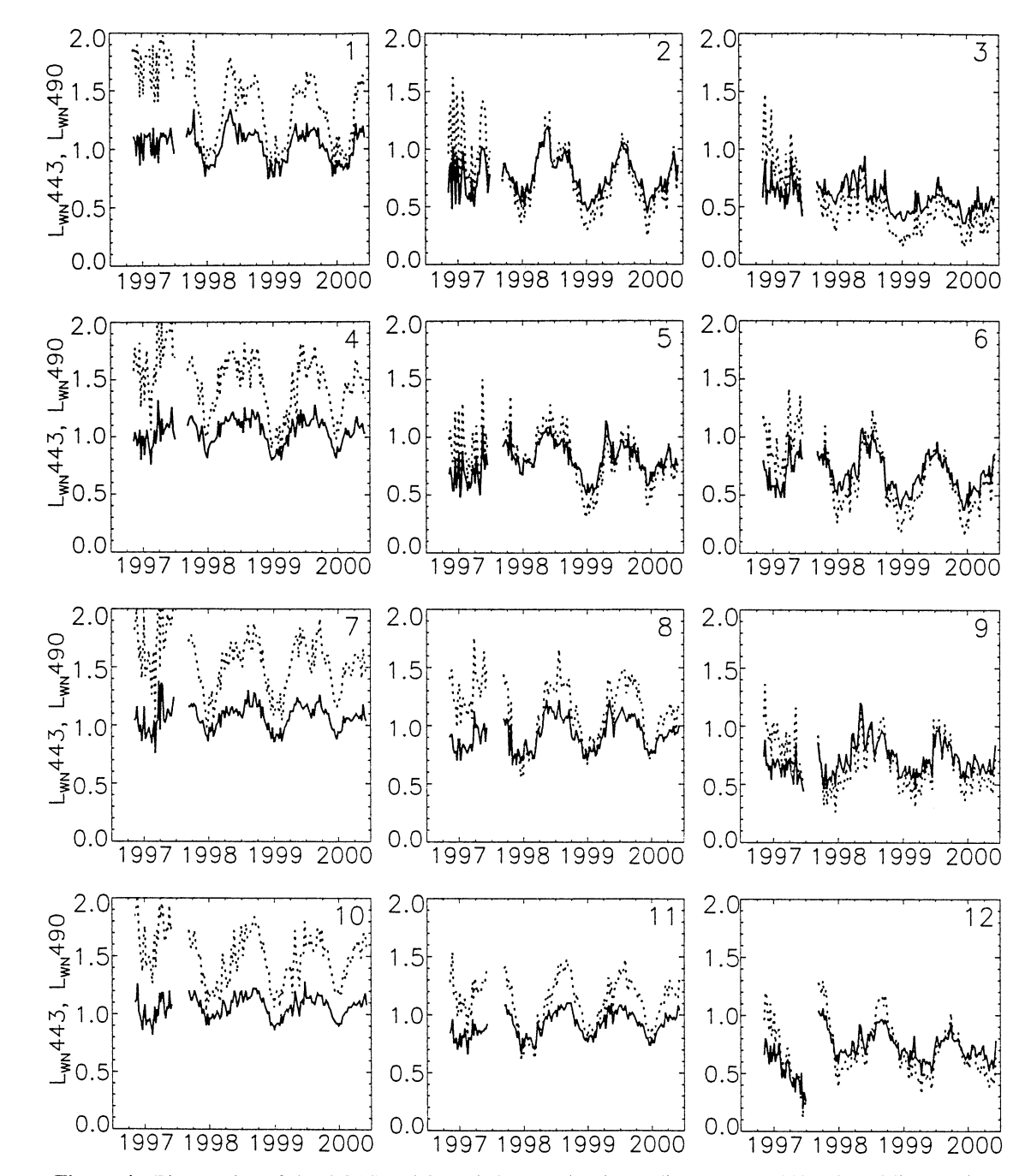


Figure 4. Time series of the OCTS and SeaWiFS water-leaving radiances $L_{\rm WN}$ (443) (dotted line) and $L_{\rm WN}$ (490) (solid line) in μ W cm⁻² μ m⁻¹ sr⁻¹. OCTS data cover a period from late 1996 to mid-1997. On this and the following plots, a panel is located according to the location of the subarea in Figure 1, and the number in the upper right corner is the subarea number. The year labels are centered at January 1 of the respective year.

analyze all the differences between different versions of the SeaWiFS data, but it is important to note that changes in processing algorithms and calibrations will affect further versions of the satellite time series.

4.2. Chlorophyll

Chl time series for the subareas derived with the CAL-P6 algorithm (with spectrally adjusted coefficients for OCTS) are shown in Figure 5. The standard NASA SeaWiFS 8-day Chl product (version 2) derived by compositing level 2 data and

using OC2v2 algorithm yielded a qualitatively similar time series to our CAL-P6 time series but at approximately 15% lower levels (overall median, range for the medians of the subareas from 11% to 31%). The underestimation of the OC2v2 algorithm relative to in situ Chl in the California Current was the main reason why the CAL-P6 algorithm was developed [*Kahru and Mitchell*, 1999]. We also applied the OC2v2 algorithm to binned radiances and compared the results with the standard NASA Chl products. It appears that the effect of applying the Chl algorithm to binned 8-day

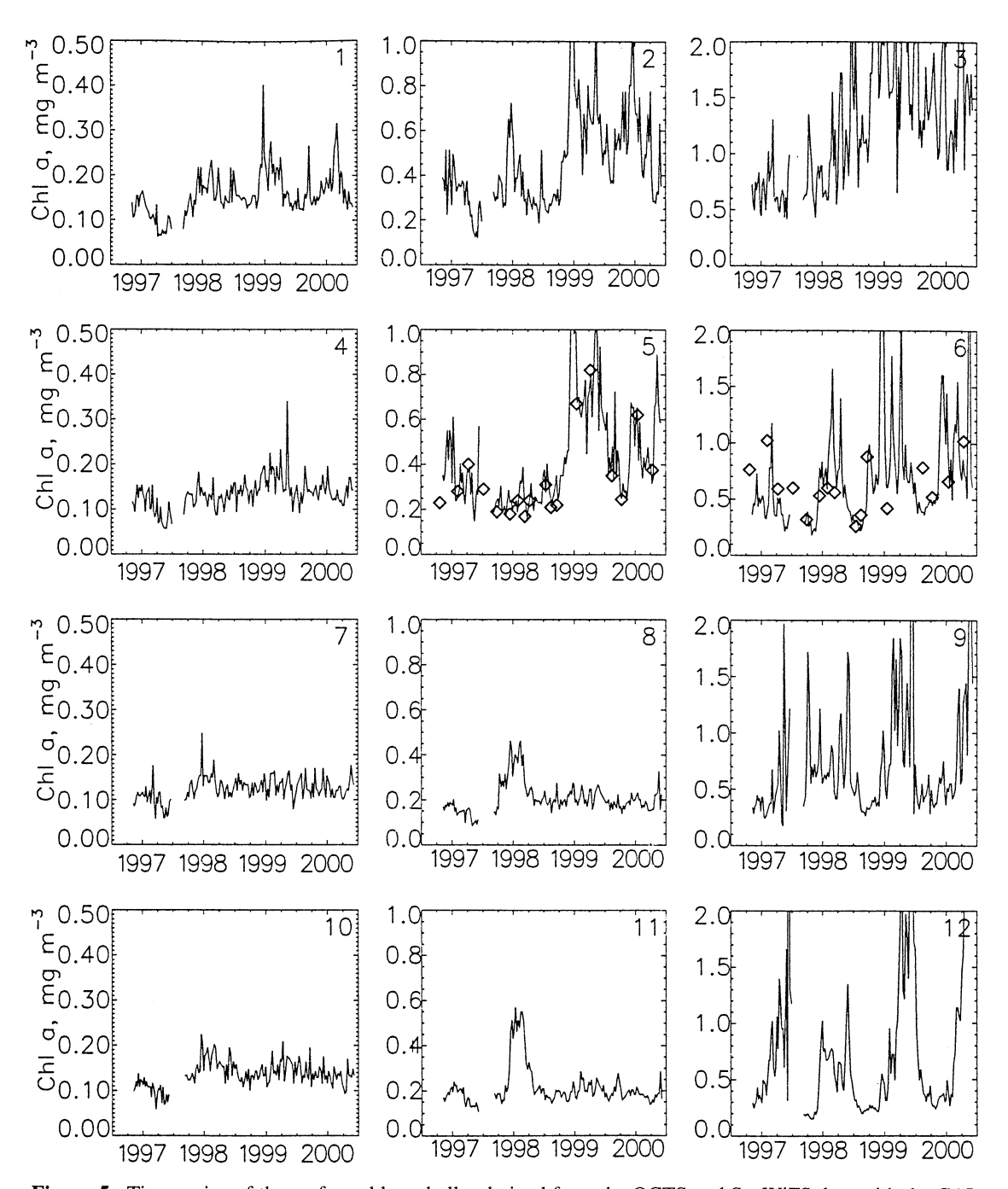


Figure 5. Time series of the surface chlorophyll *a* derived from the OCTS and SeaWiFS data with the CAL-P6 algorithm. Median in situ values (diamonds) from CalCOFI cruises are shown for subareas 5 and 6. Note the change in scale from offshore to inshore bands.

radiances as compared to applying the same algorithm at unbinned level 2 data reduced the median Chl by about 10%. The error was similar when applied to daily binned radiances and slightly bigger (13% median) when applied to monthly binned radiances. These errors were largest in the highly variable coastal zone (subarea 3). In conclusion, the errors due to application of the algorithms to binned data versus unbinned data are of the order of 10% and relatively minor in comparison with other errors (e.g., atmospheric correction). It was more important to use the same locally validated algorithm for both sensors in order to be able to combine

results from the two satellite sensors. The monthly Chl averages for each subarea calculated with the CAL-P6 algorithm showed no significant bias between OCTS and SeaWiFS version 2 data. The increase in SeaWiFS $L_{\rm WN}$ (555) values in version 3 resulted in increased SeaWiFS Chl estimates. Therefore, the monthly mean OCTS Chl is lower than the corresponding SeaWiFS Chl in many areas. It is difficult to assess how much of the difference is due to algorithm issues and how much is due to real increases in the surface Chl over time.

The satellite estimates are based on median values over

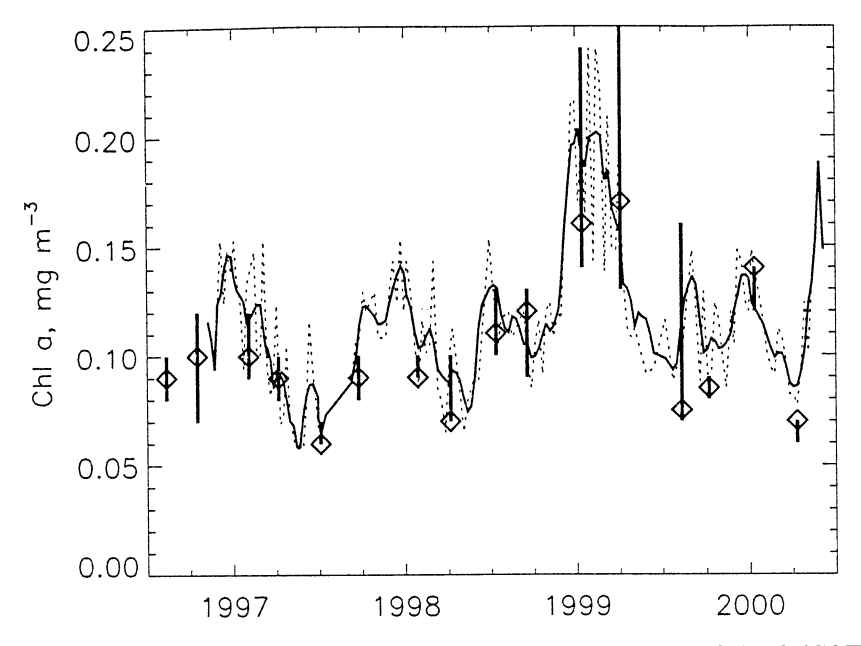


Figure 6. Time series of the surface chlorophyll *a* in the southwest corner of the CalCOFI station grid (center of subarea 4). Ship-based measurements include the median (diamond) and minimum-maximum range (vertical line) from CalCOFI cruises. Satellite estimates show medians from 8-day composited SeaWiFS images (version 3, OC4v4 Chl algorithm, dotted line) and those smoothed with a polynomial low-pass filter (solid line).

many (at least 100, usually hundreds or thousands) cloud-free pixels and should therefore be good estimates of the mean concentration. However, the location of cloud-free pixels within the subarea is variable from image to image and causes some of the observed variability. In contrast, in situ measurements are based on a small number of stations per subarea and are affected by the small-scale spatial and temporal variability. As the location of cloud-free pixels within the subarea does not necessarily coincide with the location of stations, discrepancies between the in situ and satellite measurements are inevitable. The correspondence between satellite and in situ time series of Chl is better offshore with less variability compared with the highly variable inshore areas (compare areas 5 and 6 in Figure 5). As near-simultaneous (within ±4 hours, ±1 km) match-ups show good correlation and no significant bias (Figure 2), we expect the satellite and in situ time series to agree well when the area is relatively homogeneous and sufficient cloud-free images and in situ data are available. To reduce the effect of spatial mismatch between satellite and in situ measurements, we selected a small validation area (327 pixels) in the SW corner of the CalCOFI station grid (center of subarea 4 in Figure 1, CalCOFI stations 90.110, 90.120, 93.110, 93.120) with minimal space-time variability. We used SeaWiFS version 3 Chl data (OC4v4 algorithm applied to binned radiances). The validation results (Figure 6) show that while there is no significant bias between the satellite and in situ time series, the correspondence is not better in comparison with the much larger subarea 5 (4828 pixels) using CAL-P6 algorithm applied to binned radiances (Figure 5, panel 5). We believe that the main reason for that is the range of Chl, which is 4-5 times higher in area 5. At very low Chl the inherent digitization errors of the instrument and errors of the atmospheric correction are more important than those at midrange Chl (Hu et al., in press). Considering these limitations, we cannot detect any significant bias between the in situ and satellite measurements.

Offshore and outer shelf areas show indications of winter (December-March) Chl maxima at least in some years, while the inshore waters tend to have extended spring-early summer maxima (January-June). All regions tend to have annual late summer minima. However, intermittent blooms at shorter timescales as well as interannual variability tend to mask the seasonal periodicity. Satellite-detected time series show a trend of increasing Chl for the central and southern California zones (subareas 1-6) and inshore southern Baja (subarea 12), which is significant (at 95% confidence limit using the Sen slope indicator) for both the combined OCTS-SeaWiFS and only SeaWiFS time series. The Chl maxima in all these areas were associated with the strong La Niña and cold waters in 1999.

4.3. CDOM

Compared with Chl, both the time and space variability of CDOM (Figure 7) is much less: the total variation range of the subarea medians is about five-fold compared with the approximately 40-fold Chl variation. Because of the smaller variability and smoother changes, the CDOM annual time series can be sampled at monthly intervals instead of our standard weekly intervals with no significant loss of detail. Most of the spikes in the weekly time series are probably due to limited coverage because of the clouds. A comparison with in situ data shows good correspondence of the SeaWiFS estimates in subareas with good station coverage (Figure 8) but OCTS under-estimates (data not shown). The cause of the OCTS underestimation is not known: it could be attributed to several factors, including errors in our in situ methods, a bias

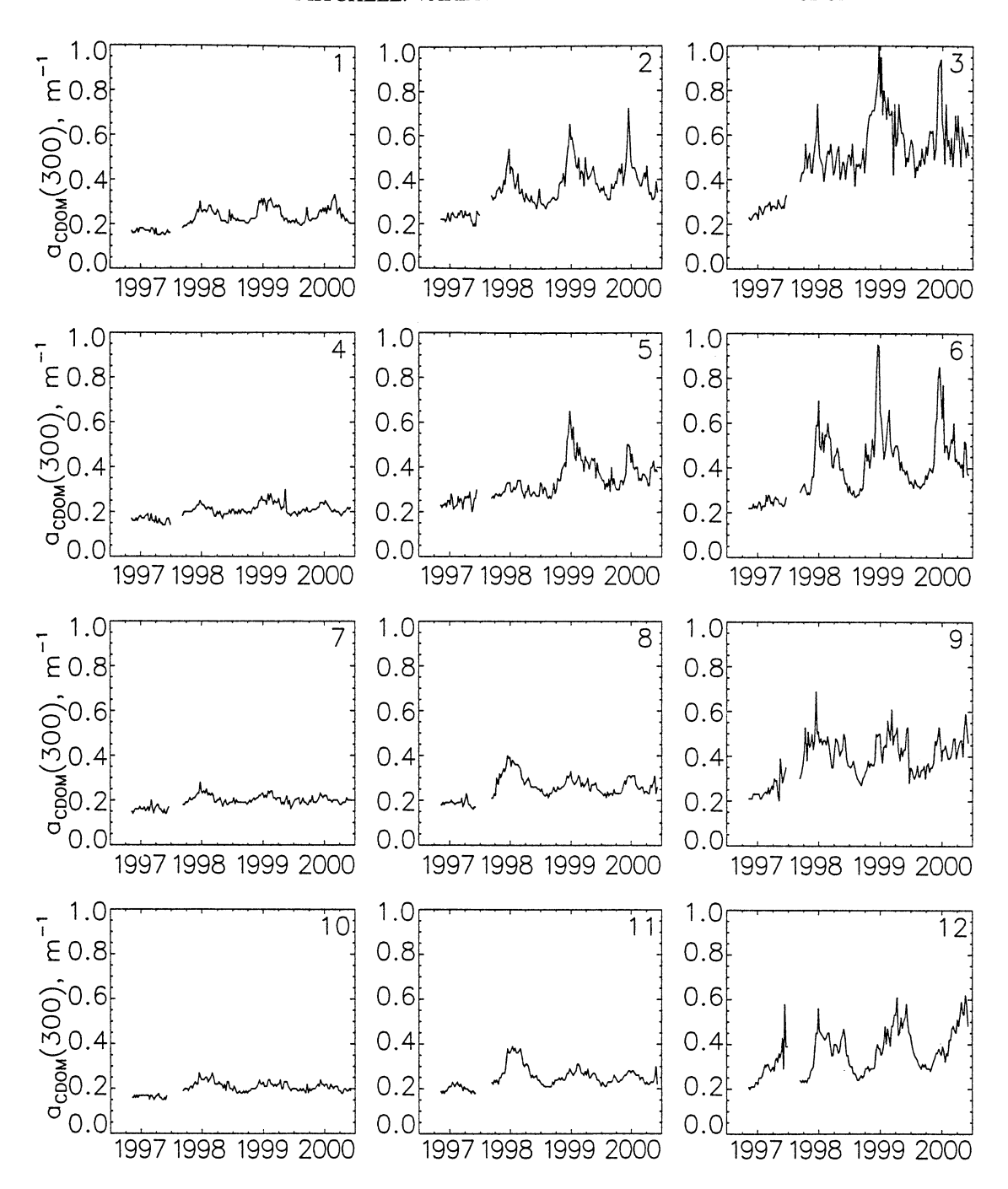


Figure 7. Time series of CDOM absorption at 300 nm derived from the OCTS and SeaWiFS data using the $L_{WN}(443)/L_{WN}(510)$ ratio (Figure 3; Table 1).

in the OCTS $L_{\rm WN}$ data, algorithm errors, or a combination of these. Annual CDOM cycle with maxima during winterspring (December-May) and minima during late summer (around August) is evident in SeaWiFS data, especially for inshore regions. The corresponding winter maximum is not evident in the short OCTS time series, except in area 11. The maxima for inshore waters are extended or shifted toward spring and early summer (areas 6, 9, 12). Even when excluding OCTS and using only the SeaWiFS data, a significant trend (at 95% confidence limit) of increasing CDOM can be detected in subareas 2, 3, 5, 6, 12. The same areas had a positive trend of Chl as well.

4.4. Comparison Between Empirical and Semianalytic Algorithms

In addition to the time series derived with our empirical Chl and CDOM algorithms, we also calculated similar time series with the *Carder et al.* [1999] semianalytic algorithm. Qualitatively the algorithms showed good agreement in most cases. At moderate and high Chl (approximately ≥1.5 mg m⁻³) the semianalytic algorithm failed and a comparison was not possible. Compared with our empirical algorithms, the semianalytic algorithm underestimated Chl and overestimated CDOM. This discrepancy is at least partly caused by the

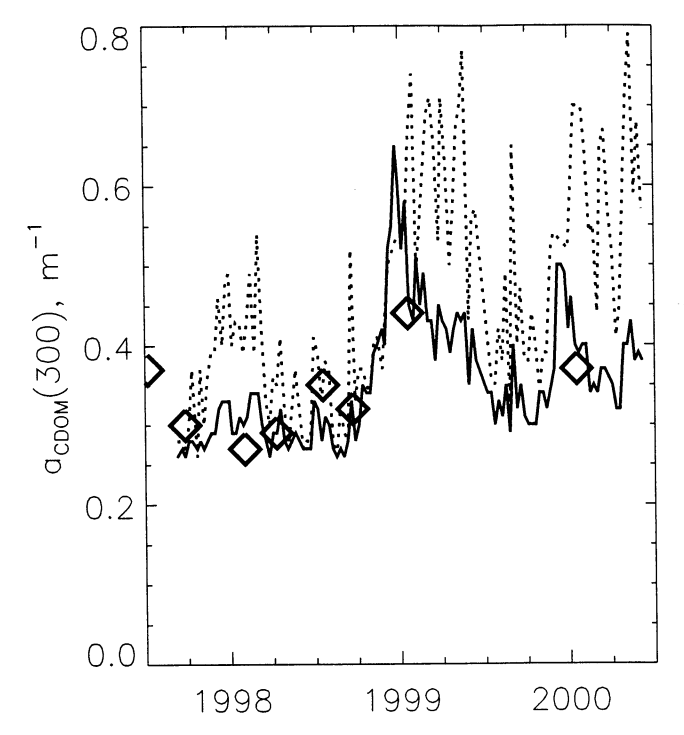


Figure 8. CDOM time series in subarea 5 derived from SeaWiFS data using the $L_{\rm WN}$ (443)/ $L_{\rm WN}$ (510) ratio (solid line) and the *Carder at al.* [1999] semianalytic algorithm (dotted line). Median in situ values (diamond) from CalCOFI cruises are overlaid.

errors in the atmospheric correction of the 412-nm band [Barnard et al., 1998; Kahru and Mitchell, 1999; Siegel et al., 2000]. However, quantitative differences between the algorithms can result in different seasonal patterns (Figure 9).

The semianalytic algorithm produced a strongly enhanced winter maximum in CDOM (especially in subareas 8 and 11) and showed no corresponding Chl maximum, whereas the empirical algorithms produced winter maxima in both Chl and CDOM. We have no in situ data to evaluate these discrepancies in the satellite algorithms for subareas 8 and 11. However, Mexican cruises during winter 1997-1998 to this region did find higher than normal Chl in subarea 11 (G. Gaxiola, pers. Comm.).

4.5. Seasonal Periodicity and Interannual Variations

Seasonal periodicity in Chl and CDOM is evident for most subareas at least for some years. However, the seasonal cycle is often masked by variability on both shorter and longer timescales. Variance spectra calculated for the combined OCTS-SeaWiFS time series of both Chl and CDOM confirmed the existence of the dominant annual variability (spectra not shown). The existence of a dominant spectral peak at periods close to 1 year was significant (at 99% confidence limit) for most of the subareas. Spectral peaks at higher frequencies were variable between different subareas. The Lomb periodograms for the SeaWiFS CDOM time series showed a dominant annual period in all subareas. Only in area 5 did the interannual component exceed the annual component. The variability in Chl had broader temporal distribution, but a significant annual peak was found in most subareas (Figure 10). To evaluate the effect of different algorithms and processing methods, we applied the Lomb periodogram analysis to Chl time series derived by applying CAL-P6 to binned radiances and OC4v4 to unbinned radiances. Differences between the methods were evident in subarea 3 with the highest spatial and temporal variability and in subarea 7 with the least variability and were relatively minor in other areas. The interannual variability component

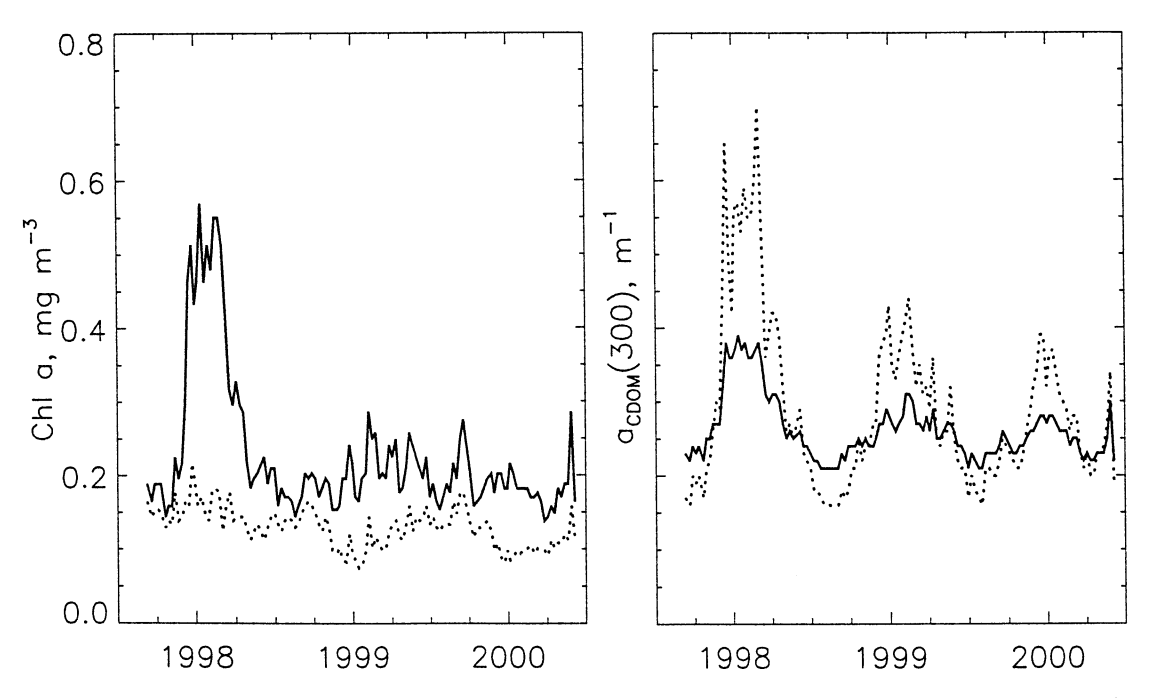


Figure 9. Chl and CDOM time series in subarea 11 derived from SeaWiFS data with the *Carder at al.* [1999] semianalytic algorithm (dotted lines) and our CAL-P6 algorithm for Chl and the band ratio algorithm from CDOM (solid lines).

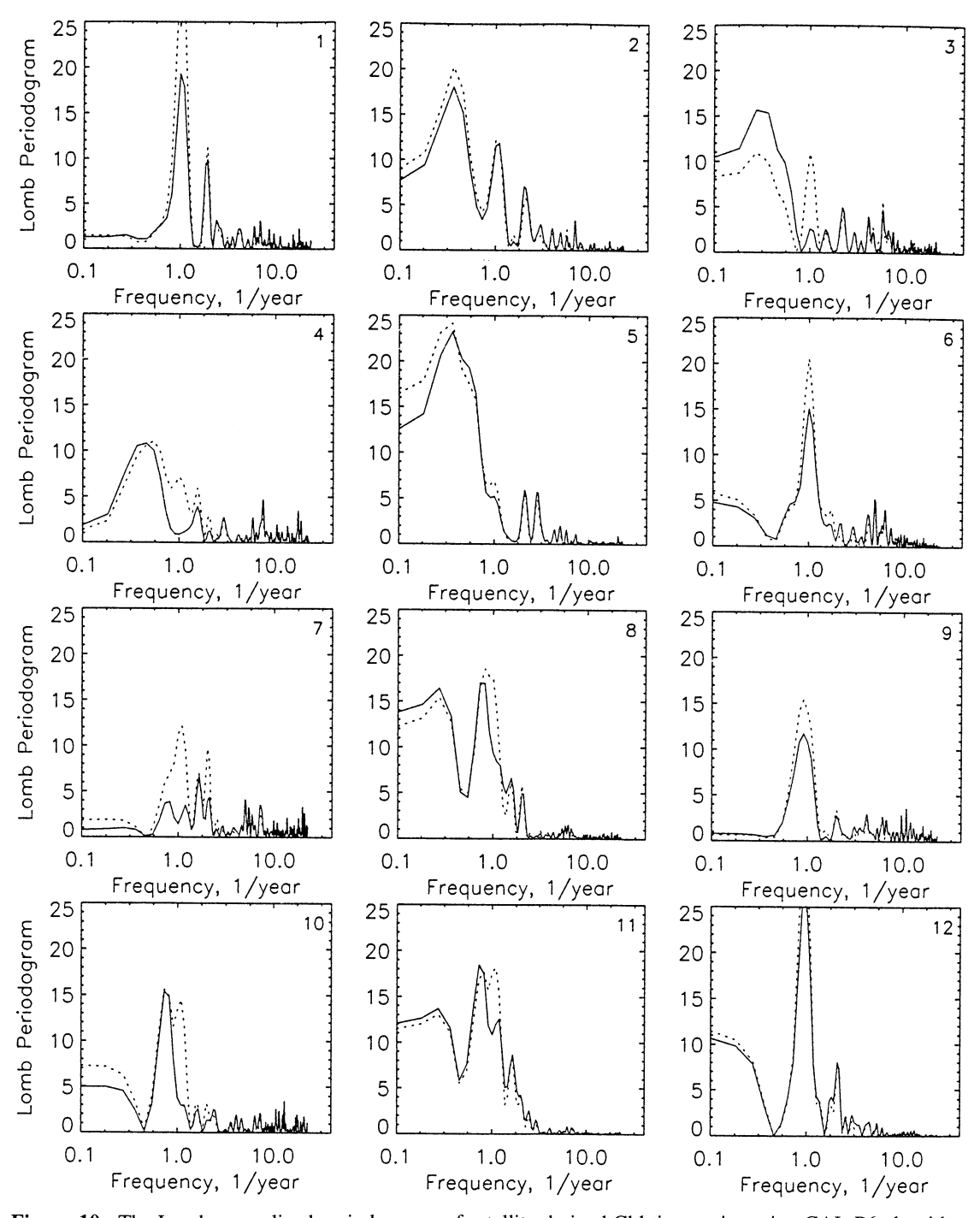


Figure 10. The Lomb normalized periodograms of satellite-derived Chl time series using CAL-P6 algorithm (applied to binned version 3 $L_{\rm WN}$ data from SeaWiFS, solid line) and OC4v4 (applied to level 2 $L_{\rm WN}$, dotted line).

was dominant in areas 2, 3, 4, and 5. Periodograms of areas 8 and 11 showed distinct peaks at both annual and interannual frequencies.

5. Discussion

The early studies of Chl distribution using the CZCS West Coast Time Series [Abbott and Zion, 1985] showed strong winter maxima and summer minima [e.g., Michaelson et al., 1988], but the winter maxima were later disputed as being caused by errors due to the single-scattering atmospheric

correction algorithm [Thomas and Strub, 1990; Strub et al., 1990]. The empirical correction proposed by Strub et al. [1990] removed the winter Chl maximum by subtracting the first empirical orthogonal function of the offshore variability. This assumed that the offshore chlorophyll concentration was essentially constant and produced a reversed cycle with a "strong" spring-summer maximum. The improved atmospheric correction that was implemented in the reprocessed global CZCS data [Feldman et al., 1989] reduced or removed the exaggerated offshore winter Chl maximum. Thomas et al. [1994], using the reprocessed CZCS data claim

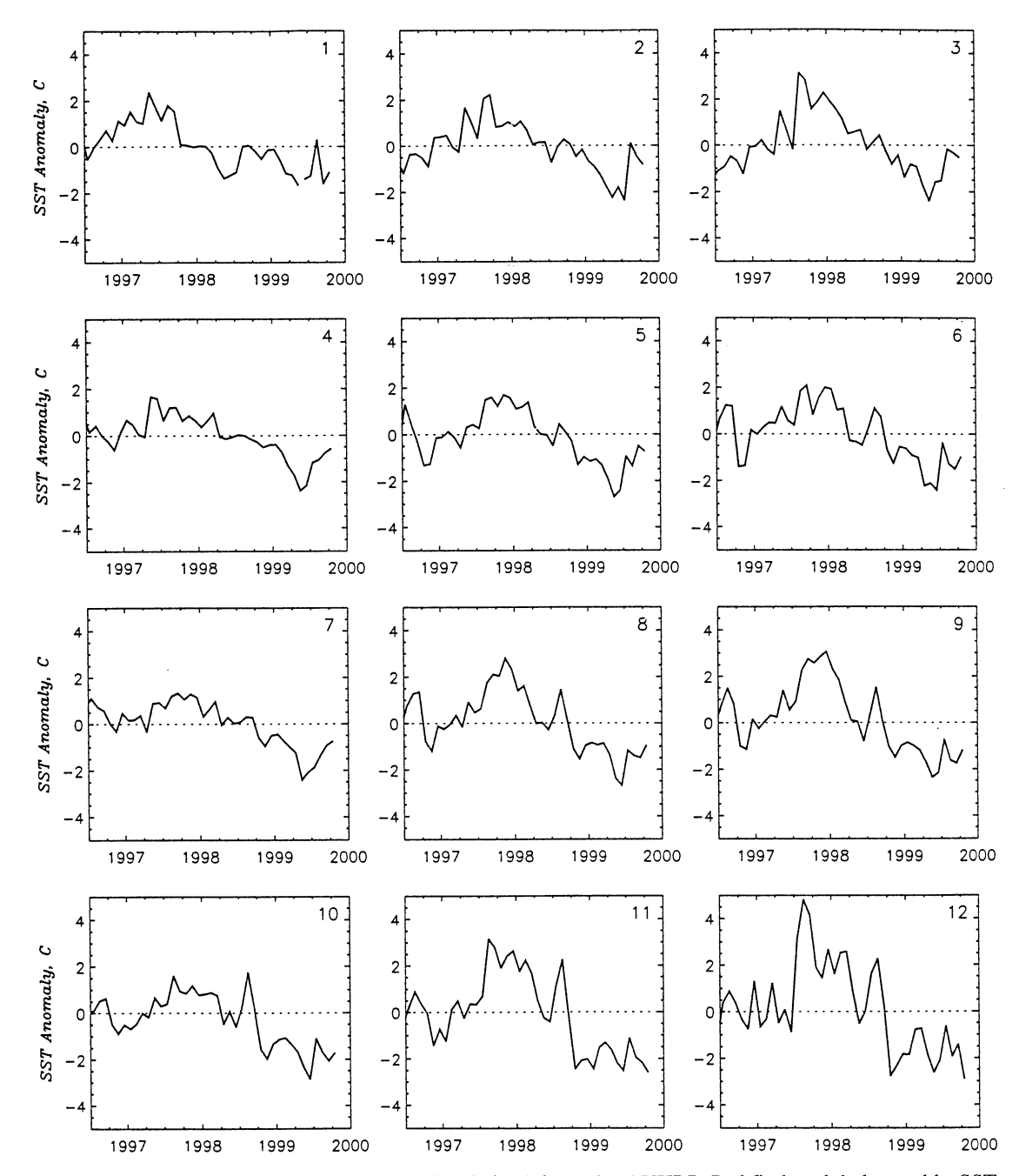


Figure 11. Sea surface temperature anomalies derived from the AVHRR Pathfinder global monthly SST maps.

summer maxima within 100 km of the coast ("strongest" in two latitude ranges, 34°N-45°N and 24°N-29°N) and a "diffuse" winter maximum offshore.

The data available from the new generation of ocean color sensors (OCTS, SeaWiFS, and others) do not yet match the length of the 1978-1986 CZCS time series but provide a more dense (every second day locally) series of images with improved sensor characteristics and processing algorithms. In this paper we have shown that satellite estimates of surface Chl in the California Current agree well with in situ measurements. Observed discrepancies between satellite and in situ time series of Chl are mostly due to different spatial and temporal coverage of these very different methods. We did not detect any significant bias between satellite and ship-

based surface Chl estimates. The validation for in-shore waters must be considered preliminary, as reliable validation is difficult to perform in the highly variable coastal waters. Satellite measurements are not possible during overcast or foggy situations; therefore bias between satellite and in situ time series may be introduced by missing satellite measurements during these periods.

Semianalytic algorithms using all available bands to derive in-water properties [Garver and Siegel, 1997; Carder et al., 1999] may eventually derive more products with better accuracy than simple band ratio algorithms, but current versions are very sensitive to parameterization and atmospheric correction errors, especially at short wavelengths.

Based on the new satellite-derived time series of about 3.5

years, we have shown that the annual cycle is present in both Chl and CDOM but is often overshadowed by interannual variability (El Niño-La Niña cycle) as well as by highfrequency variability. Late summer minima in both parameters were consistently observed for most regions. The seasonal pattern was also observed off southern California, where Thomas et al. [1994] did not detect significant seasonality. CDOM had winter maxima and late summer minima during most of the examined years. For inshore waters the rapid increase during winter months was also present, but the maxima extended through spring until early summer. The Chl time series showed winter maxima during some years and in some subareas, while for other areas and years the maxima were not present or barely detectable. For example, during the 1998 El Niño the winter Chl maximum was missing in the southern California outer shelf (area 5) but was enhanced in the neighboring Baja subareas 8 and 11. During the winter of 1999 the situation was reversed, and the southern California outer shelf had a strong winter maximum. Indications of winter Chl maxima offshore can also be seen in the CalCOFI in situ data (e.g., Figure 6). Chavez [1995] showed that the winter Chl maxima off central California are caused by increased phytoplankton biomass due to higher nutrient fluxes and increased chlorophyll per cell, whereas the redistribution of the deep chlorophyll maximum to the surface by vertical mixing is of minor importance.

The time period analyzed here included the 1997-1998 El Niño [Chavez et al., 1999] and the following strong La Niña. The 1982-1983 El Niño caused a reduction of upwelling and surface Chl in the California Current [Fiedler, 1984]. We detected a significant reduction in the extent of the eutrophic (Chl >1 mg m⁻³) waters along the coast and an increase in the extent of mesotrophic (0.2 < Chl \leq 1 mg m⁻³) waters off Baja California during the 1998 El Niño [Kahru and Mitchell, 2000]. Here we show satellite evidence of an increasing trend for both Chl and CDOM in many subareas that are likely to be related to the multiannual forcing. The validity of the satellitedetected increase in Chl and CDOM concentrations is also supported by the anomalous sea surface temperature variability. The SST time series showed that from 1997 to 1999 the system changed abruptly from one of warmest months (since 1981) to one of the coldest months for the almost 20-year SST time series. Figure 11 shows that the positive SST anomalies of 2°-4°C in late 1997 gradually turned into approximately 2°C negative anomalies in mid-1999 for all the inshore areas. The SST has remained below the long-term mean for most subareas through December 1999, and SeaWiFS estimates of Chl and CDOM remained relatively high off central and southern California.

The satellite-detected CDOM concentration seems to be a promising parameter for detecting seasonal and interannual changes because it exhibits significantly smaller time and space variability compared with Chl. Summer minima and winter maxima similar to the annual cycle of CDOM in the California Current have been detected in the Sargasso Sea by in situ measurements of light attenuation [Siegel and Michaels, 1996]. However, in the Sargasso Sea the concentration of "colored dissolved or detrital material" is not correlated with Chl, and its dynamics is believed to be controlled by photo-oxidation near the surface and production at depth. In the California Current our satellite-derived estimate of CDOM absorption is well correlated with Chl in

the offshore and outer shelf waters and not well correlated in the inshore waters. These observations support the hypothesis that in the offshore waters CDOM is produced by phytoplankton and therefore well correlated with chlorophyll, whereas in the coastal zone other sources (land or bottom) become dominant.

Acknowledgments. This work was supported by the NASA Ocean Biogeochemistry (NAG5-6559) and NASA SIMBIOS (NAS5-97130) programs. We thank the CalCOFI program for in situ Chl data, the SeaWiFS Project and the Distributed Active Archive Center at NASA Goddard Space Flight Center for the SeaWiFS data, the Remote Sensing Technology Center of Japan (NASDA) for the OCTS data, and the Jet Propulsion Laboratory (NASA) for SST data.

References

- Abbott, M. R., and P. M. Zion, Satellite observations of phytoplankton variability during an upwelling event, *Cont. Shelf Res.*, 4, 661-680, 1985.
- Barnard, A. H., J. R. V. Zaneveld, J. L. Mueller, W. S. Pegau, and C. Trees, SeaWiFS ocean color in the Gulf of California: variability, validation and algorithm development. Paper presented at Ocean Optics XIV, ONR/NASA, Kailua Kona, Hawaii, Nov. 10-13, 1998.
- Bernal, P. A., and J. A. McGowan, Advection and upwelling in the California Current, in *Coastal Upwelling, Coastal Estuarine Sci.*, vol. 1, edited by F. A. Richards, pp. 381-399, AGU, Washington, D. C., 1981.
- Bricaud, A., A. Morel, and L. Prieur, Absorption by dissolved organic matter of the sea (yellow substance) in the UV and visible domains, *Limnol. Oceanogr.*, 26, 43-53, 1981.
- Campbell, J. W., J. M. Blaisdell, and M. Darzi, Spatial and temporal binning algorithms, NASA Tech. Memo. 32 (104566), 73 pp., 1995
- Carder, K. L., F. R. Chen, Z. P. Lee, and S. K. Hawes, Semianalytic Moderate-Resolution Imaging Spectrometer algorithms for chlorophyll a and absorption with bio-optical domains based on nitrate depletion temperatures, J. Geophys. Res., 104, 5,403-5,421, 1999.
- Chavez, F. P., A comparison of ship and satellite chlorophyll from California and Peru, *J. Geophys. Res.*, 100, 24,855-24,862, 1995.
- Chavez, F. P., P. G. Strutton, G. E. Friederich, R. A. Feely, G. C. Feldman, D. G. Foley, and M. J. McPhaden, Biological and chemical response of the equatorial Pacific Ocean to the 1997-98 El Niño, *Science*, 286, 2,126-2,131, 1999.
- Chelton, D. B, P. A. Bernal, and J. A. McGowan, Large-scale interannual physical and biological interaction in the California Current, J. Mar. Res., 40, 1,095-1,125, 1982.
- Dettinger, M. D., M. Ghil, C. M. Strong, W. Weibel, and P. Yiou, Software expedites singular-spectrum analysis of noisy time series, *Eos Trans. AGU*, 76, 12, 14, 21, 1995.
- Fargion, G. S., J. A. McGowan, and R. H. Stewart, Seasonality of chlorophyll concentrations in the California Current: A comparison of two methods, *Calif. Coop. Ocean. Fish. Invest.* Rep., 34, 35-50, 1993.
- Feldman, G. C., N. Kuring, C. Ng, W. Esaias, C. McClain, J. Elrod, N. Maynard, and D. Endres, Ocean color - availability of the global data set, *Eos Trans. AGU*, 70, 634-635, 640-641, 1989.
- Fiedler, P. C., Satellite observations of the 1982-1983 El Niño along the U.S. Pacific coast, *Science*, 224, 1,251-1,254, 1984.
- Franz, B., OCTS, MOS, and POLDER vicarious calibration analyses, Paper presented at SIMBIOS Science Team Meeting, NASA, Annapolis, MD, Sept. 13, 1999.
- Fu, G., K. Settle, and C. R. McClain, SeaDAS: The SeaWiFS Data Analysis System, in *Proceedings of the Fourth Pacific Ocean Remote Sensing Conference, Qingdao, China*, pp. 73-77, 1998.
- Garver, S. A., and D. A. Siegel, Inherent optical property inversion of ocean color spectra and its biogeochemical interpretation, 1, Time series from the Sargasso Sea, *J. Geophys. Res.*, 102, 18,607-18,625, 1997.
- Gilbert, R. O., Statistical Methods for Environmental Pollution Monitoring, Van Nostrand Reinhold, New York, 1987.
- Hayward, T. L., et al., The state of the California Current in 1998-

- 1999: Transition to cool water conditions, Calif. Coop. Ocean. Fish. Invest. Rep., 40, 29-62, 1999.
- Hu, C., K. L. Carder, and F. E. Müller-Karger, How precise are SeaWiFS ocean color estimates? Implications of digitizationnoise errors, Remote Sens. Environ. (In press).
- Kahru, M., and B. G. Mitchell, Empirical chlorophyll algorithm and preliminary SeaWiFS validation for the California Current. *Int. J. Remote Sens.*, 20, 3,423-3,429, 1999.
- Kahru, M., and B. G. Mitchell, Influence of the 1997-98 El Niño on the surface chlorophyll in the California Current, *Geophys. Res. Lett.*, 27, 2,937-2,940, 2000.
- Lomb. N. R., Least-squares frequency analysis of unequally spaced data, *Astrophys. Space Sci.*, 39, 447-462, 1976.
- Lynn, R. J, and J. J. Simpson, The California Current system: The seasonal variability of its physical characteristics, J. Geophys. Res., 92, 12,947-12,966, 1987.
- McClain, C. R., Review of major CZCS applications: US case studies, in *Ocean Colour: Theory and Applications in a Decade of CZCS Experience*, edited by V. Barale and P. M. Schlittenhardt, pp. 167-188, Kluwer Acad., Norwell, Mass., 1993.
- McClain, C. R., M. L. Cleave, G. C. Feldman, W. W. Gregg, S. B. Hooker, and N. Kuring, Science quality SeaWiFS data for global biosphere research, Sea Technol., 39, 10-16, 1998.
- Michaelsen, J., X. Zhang, and R. C. Smith, Variability of pigment biomass in the California Current system as determined by satellite imagery, 2, Temporal variability, J. Geophys. Res., 93, 10,883-10,896, 1988.
- Mitchell, B. G., and M. Kahru, Algorithms for SeaWiFS standard products developed with the CalCOFI bio-optical data set, *Calif. Coop. Ocean. Fish. Invest. Rep.*, 39, 133-147, 1998.
- Mitchell, B. G., et al., Determination of spectral absorption coefficients of particles, dissolved material and phytoplankton for discrete water samples, in G. S. Fargion and J. L. Mueller Ocean Optics Protocols for Satellite Ocean Color Sensor Validation, Revison 2, G. S. Fargion and J. L. Mueller, Eds., NASA Tech. Memo., 209966, NASA Goddard Space Flight Center, Greenbelt, Maryland, 2000
- O'Reilly, J. E., S. Maritorena, B. G. Mitchell, D. A. Siegel, K. L. Carder, S. A. Garver, M. Kahru, and C. R. McClain, Ocean color chlorophyll algorithms for SeaWiFS, *J. Geophys. Res.*, 103, 24.937-24,953, 1998.
- O'Reilly, J. E. et al., Ocean color chlorophyll *a* algorithms for SeaWiFS, OC2, and OC4: Version 4, in O'Reilly, J. E. et al.,

- SeaWiFS Postlaunch Calibration and Validation Analyses, Part 3, S. B. Hooker and E. R. Firestone, Eds., *NASA Tech. Memo.* 206892, Vol. 11, 9-23, NASA Goddard Space Flight Center, Greenbelt, Maryland, 2000
- Press, W. H., S. A. Tuekolsky, W. T. Wettering, and B. P. Flannery, Numerical Recipes in C: The Art of Scientific Computing, 2nd ed., 994 pp., Cambridge Univ. Press, New York, 1992.
- Siegel, D. A., and A. F. Michaels, Quantification of non-algal light attenuation in the Sargasso Sea: Implications for biogeochemistry and remote sensing, *Deep Sea Res.*, *Part II*, 43, 321-345, 1996.
- Siegel, D. A., M. Wang, S. Maritorena, and W. Robinson, Atmospheric correction of satellite ocean color imagery: the black pixel assumption, Appl. Opt., 39, 3,582-3,591, 2000.
- Strub, P. T. C. James, A. C. Thomas, and M. R. Abbott, Seasonal and nonseasonal variability of satellite-derived surface pigment concentration in the California Current, J. Geophys. Res., 95, 11,501-11,530, 1990.
- Thomas, A. C., and P. T. Strub, Seasonal and interannual variability of pigment concentration across a California Current frontal zone, *J. Geophys. Res.*, 95, 13,023-13,042, 1990.
- Thomas, A. C., F. Huang, P. T. Strub, and C. James, Comparison of the seasonal and interannual variability of phytoplankton pigment concentrations in the Peru and California Current systems, *J. Geophys. Res.*, 99, 7,355-7,370, 1994.
- Vazquez, J., A. Tran, S. Sumagaysay, E. A. Smith, and M. Hamilton, NOAA/NASA AVHRR oceans Pathfinder sea surface temperature data set user's guide, version 1.2, JPL Tech. Rep., 55, Jet Propul. Lab., Pasadena, Calif., 1995.
- Venrick, E. L., and T. L. Hayward, Determining chlorophyll on the 1984 CalCOFI surveys, Calif. Coop. Ocean. Fish. Invest. Rep., XXV, 74-79, 1984.
- Wang, M., B. Franz, A. Isaacman, C. Pietras, B. Schieber, P. Smith, T. Riley, G. Feldman, and S. Baily, SIMBIOS project activities (1997-1998), NASA Tech. Memo., 208645, 15-18, March 1999.

(Received October 10, 1999; revised August 16, 2000; accepted October 11, 2000.)

M. Kahru and B. G. Mitchell, Scripps Institution of Oceanography, University of California, San Diego, La Jolla, CA 92093-0218. (mkahru@ucsd.edu; gmitchell@ucsd.edu)